sustainability

MDPI

Article

Land Use Change and Sustainable Urban Transition Under Multi-Scenario Simulation: Policy Insights from Beijing's Ecological Conservation Area

Enquan Zhao [1], Xiaodong Liu [2,*], Jie Bai [2,*], Ming Li [2], Xiaoyang Wang [1] and Yang Zhao [1]

[1] Langfang Integrated Natural Resources Survey Center, China Geological Survey, Tianjin 300304, China; zhaoenquan@mail.cgs.gov.cn (E.Z.)
[2] Natural Resources Comprehensive Survey Command Center, China Geological Survey, Beijing 100055, China; liming_dqwl@mail.cgs.gov.cn
* Correspondence: liuxiaodong@mail.cgs.gov.cn (X.L.); baijie23@mail.cgs.gov.cn (J.B.)

Abstract

Rapid urbanization and mega-events have reshaped land use in Beijing's Yanqing District, making post-event balance between ecological protection and urban development a critical challenge for territorial spatial planning. This study analyzes land use evolution from 2015 to 2025, simulates 2035 patterns under natural development (ND), ecological protection (EP), and urban development (UD) using the PLUS model (Kappa = 0.91, OA = 0.95), and constructs an Ecological Conversion Direction Index (*ECDI*) to characterize the net direction of ecological quality change. Results show forest and construction land increased (+40.17 km^2; +14.83 km^2), grassland declined sharply (−38.23 km^2, −36.47%), cropland decreased (−25.36 km^2, −5.17%), and water expanded (+8.59 km^2, +62.38%). The *ECDI* remained positive (0.313 to 0.178) but weakened post-event. The driving mechanism showed a trend of transition from "event-response" toward "ecological constraint"—the contribution of distance to landmarks/venues declined substantially for most land types, while NDVI emerged as a prominent predictor negatively associated with construction land (18.24%) and positively associated with forest quality improvement (17.55%). The EP scenario was identified as optimal, reducing construction land by 8.05 km^2 to 98.67 km^2 while increasing forest to 1388.57 km^2, effectively safeguarding both the ecological baseline and cropland redline. We recommend adopting EP, strengthening the construction land reclamation rate, and coordinating the three control lines. These findings provide evidence-based policy support for reconciling urban development with ecological conservation in rapidly urbanizing ecological protection areas.

Keywords: land use change; PLUS model; multi-scenario simulation; urban sustainable development; Yanqing District

Check for updates

Academic Editor: Tommaso Caloiero

Received: 6 August 2026
Revised: 3 September 2026
Accepted: 10 September 2026
Published: 19 September 2026

Copyright: © 2026 by the authors. Licensee MDPI, Basel, Switzerland. This article is an open access article distributed under the terms and conditions of the Creative Commons Attribution (CC BY) license.

1. Introduction

Land use/cover change (LUCC) is a core issue in global change research, as it directly reflects the intensity of human modification of the Earth's surface and profoundly affects regional ecological security and sustainable development capacity [1–5]. With accelerating urbanization, construction land continues to expand, while ecological land such as cropland and forest is persistently encroached upon, leading to a series of problems including declining ecosystem service functions and increasing landscape fragmentation [3,6]. Scientific simulation and prediction of future land use change trends are of great significance for

optimizing territorial spatial patterns and coordinating the relationship between protection and development.

In recent years, scholars worldwide have conducted extensive research on land use simulation, with commonly used models including CA–Markov, CLUE–S, and FLUS [7–10]. Among them, the PLUS (Patch-generating Land Use Simulation) model [11] integrates a Land Expansion Analysis Strategy (LEAS) and a Cellular Automaton model based on multi-type random patch seeds (CARS). It can effectively identify the driving mechanisms of various land use changes and accurately simulate multi-type land use transformations at the patch scale. The model has been successfully applied in regions such as Wuhan, the Beijing–Tianjin–Hebei region, and mountainous towns [1,12–22].

As cities worldwide strive to achieve the Sustainable Development Goals (SDGs), reconciling urban growth with ecological conservation has become a central challenge, particularly in peri-urban ecological protection areas [23–25]. Unlike conventional urban regions, these areas face dual pressures from external development forces and internal conservation mandates, making the identification of feasible development pathways a critical governance issue. However, existing land-use simulation studies have rarely linked scenario outcomes directly to SDG-related policy levers.

Yanqing District is located in the northwest of Beijing and serves as an important ecological conservation area and ecological barrier for the capital. In recent years, Yanqing has hosted major events including the 2019 International Horticultural Exhibition and the 2022 Winter Olympics, during which infrastructure and tourism facilities were rapidly developed, resulting in drastic changes in land use patterns [26]. At the same time, as the "northwest ecological gateway" of the capital, Yanqing undertakes important ecological functions such as water conservation, windbreak and sand fixation, and biodiversity protection [27]. How to balance ecological protection and urban development in the post-event period and achieve a sustainable transition has become a key issue in local territorial spatial planning.

Existing studies on land use in Yanqing have mostly focused on single periods or specific project impacts, lacking dynamic multi-scenario predictions and rarely linking simulation results to sustainable development pathways. To address these gaps, this study seeks to answer three specific research questions: (1) What are the spatiotemporal characteristics of land use change in Yanqing from 2015 to 2025, and how did the sequential hosting of major events—the 2019 Horticultural Exhibition and the 2022 Winter Olympics—influence the trajectory of land use transitions? (2) How did the driving mechanisms of land use expansion shift between the event-preparation period (2015–2020) and the post-event restoration period (2020–2025), and what does this shift imply for the transition from "event-response" to "ecological-constraint" governance? (3) Among the three development scenarios for 2035—natural development (ND), ecological protection (EP), and urban development (UD)—which pathway offers the most sustainable balance between ecological conservation and urban growth? This study addresses these gaps by using land use data from 2015, 2020 and 2025 with the PLUS model to simulate three development scenarios for 2035, and by evaluating the outcomes through the lens of their implications for SDG 11 (Sustainable Cities and Communities) and SDG 15 (Life on Land) [23,24]. The aim is to provide quantitative references for planning decisions in Yanqing and similar ecological conservation areas.

2. Materials and Methods

2.1. Study Area

Yanqing District is located in the northwest of Beijing, covering a total area of approximately 2009 km^2 (Figure 1). The terrain is high in the north and low in the south,

with mountains in the west and north, and plains and basins in the east and south. The average elevation is about 500 m. The climate is temperate continental monsoon, with an average annual temperature of 9.2 °C and average annual precipitation of about 470 mm. Yanqing is an important ecological conservation area in Beijing, with relatively high forest coverage and numerous natural and cultural landscapes including the Badaling Great Wall, Longqing Gorge, and Yeyahu Wetland [28]. In recent years, the construction of the Horticultural Exhibition Park, Winter Olympics venues, and supporting transportation facilities has greatly promoted regional urbanization [26].

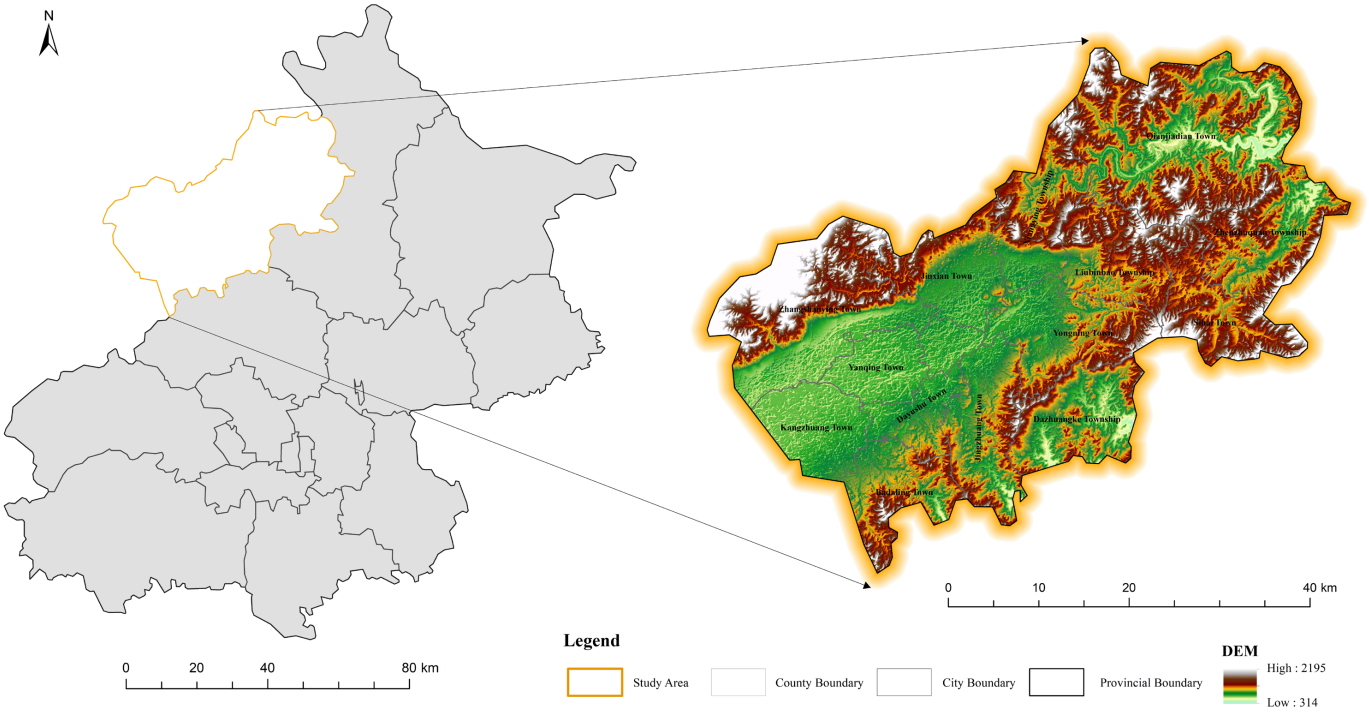

Figure 1. Location and general situation of the study area.

2.2. Data Sources

The data used in this study include land use data, topographic data, climatic data, and socioeconomic data. The sources of all data are detailed in Table 1. All data were uniformly projected to UTM WGS84 and resampled to a spatial resolution of 30 m.

The land use data are derived from the annual China Land Cover Dataset (CLCD), which provides 30 m resolution annual land cover maps for China. The CLCD was produced on the Google Earth Engine platform using 335,709 Landsat images with a random forest classifier; its overall accuracy is 79.31% based on 5463 visually interpreted samples, outperforming MCD12Q1, ESACCI_LC, FROM_GLC, and GlobeLand30 in third-party validation. The original nine CLCD classes were reclassified into five aggregated classes, with forest and shrub reclassified as forest, water and wetland as water, and barren and impervious as construction land. Cropland and grassland remained unchanged. All driving factor data were resampled to 30 m using ArcGIS 10.6 (California, USA) (Nearest Neighbor for categorical variables, Bilinear Interpolation for continuous variables) and aligned using the Snap Raster function. Distance layers were calculated using Euclidean distance.

Table 1. Data source summary.

Data Type	Resolution/Scale	Source
Administrative Boundary Road Railway River Landmarks and Venues Residential area	- 1:250,000 	Openstreetmap https://www.openstreetmap.org/ (accessed on 2 June 2026)
Elevation (m) Slope (°)	30 m 30 m	Geospatial Data Cloud https://www.gscloud.cn/search (accessed on 5 June 2026)
Land Use Type	30 m	Earth Resource Data Cloud http://www.gis5g.com/data/qxsj/ (accessed on 5 June 2026)
Mean Annual Temp. (°C) Mean Annual Precip. (mm) Gross Domestic Product (10,000 yuan/km^2)	1 km 1 km 1 km	Resource and Environmental Science Data Platform https://www.resdc.cn/DOI/ (accessed on 2 June 2026)
Population (persons/km^2)	100 m	LandScan https://landscan.ornl.gov/ (accessed on 5 June 2026)
Night Light (nW/cm^2/sr)	500 m	National Earth System Science Data Center (https://www.geodata.cn) (accessed on 2 June 2026)
NDVI	-	National Tibetan Plateau/Third Pole Environment Data Center (http://data.tpdc.ac.cn) (accessed on 2 June 2026)

2.3. Method

2.3.1. Land Use Change Analysis

Land use types were classified into five categories: cropland, forest, grassland, water, and construction land. ArcGIS 10.6 was used to calculate the area of each type for each period, construct transition matrices, and analyze the quantity and direction of land use change. To characterize the net direction of ecological quality change between two stages, this study constructed an Ecological Conversion Direction Index (*ECDI*):

$$ECDI = \frac{S_{eco_up} - S_{eco_down}}{S_{total_transfer}}$$

where S_{eco_up} is the area converted to higher ecological value land types (grassland to forest, cropland to forest, cropland to grassland, construction land to ecological land), S_{eco_down} is the area of reverse conversions (forest to cropland, forest to grassland, ecological land to construction land), and $S_{total_transfer}$ is the total conversion area. The denominator $S_{total_transfer}$ serves as a normalization factor, constraining the *ECDI* to the range $[-1, 1]$ and thereby enabling consistent comparisons across different periods, regions, or scenarios with varying total conversion scales. The *ECDI* is specifically designed to indicate the net directional tendency of ecological quality change—that is, whether up-grade conversions outweigh down-grade conversions in area—rather than the absolute magnitude of land conversion activity. An *ECDI* approaching 0 indicates that ecological improvement and degradation are approximately balanced in area, which is the intended interpretation of the index. However, because the *ECDI* does not reflect the total conversion intensity, we recommend reporting it alongside complementary metrics such as the total conversion area ($S_{total_transfer}$) or the absolute values of S_{eco_up} and S_{eco_down} for a comprehensive assessment. For instance, if $S_{eco_up} \approx S_{eco_down}$ but $S_{total_transfer}$ is very large, the *ECDI* would approach 0, correctly signaling a balanced directionality, while the large denominator would simultaneously indicate substantial landscape dynamics. Thus, the *ECDI* and

conversion intensity metrics together provide a more complete picture of land use change and its ecological implications. The *ECDI* ranges from −1 to 1, with positive values indicating ecological improvement as the dominant direction and negative values indicating ecological degradation.

2.3.2. Land Use Change Simulation (PLUS) Model

The PLUS model consists of two modules: LEAS and CARS. LEAS uses a random forest algorithm to extract the contribution rates of driving factors for the expansion of each land use type, while CARS simulates patch-level land use changes based on a roulette competition mechanism [11].

(1) Selection of Driving Factors

Referring to relevant studies [12,16] and considering the actual conditions of Yanqing, 13 driving factors were selected and classified into three categories (Table 2):

Table 2. Driving factor index system.

Category	Classification	Driving Factor	Description
Natural environment	Climatic factors	Mean Annual Precip. Mean Annual Temp.	Hydrothermal conditions affecting vegetation and agriculture
	Natural environment condition factors	Elevation Slope NDVI	Terrain elevation Degree of terrain fluctuation Vegetation cover status
Social economy	Gross Domestic Product	Gross Domestic Product	Level of economic development
	Population	Population	Intensity of human activity
	Night light	Night Light Data	Urbanization level and energy consumption
Transportation accessibility	Road	Distance to Road Distance to Railway	External rapid transit Transport artery
	Landmarks and Venues	Distance to Landmarks and Venues	Scenic areas and major facilities
	Residential area	Distance to Residential Area	Core area of human activity
	River	Distance to River	Water resource accessibility

Natural environment factors: elevation, slope, mean annual precipitation, mean annual temperature, NDVI.

Socioeconomic factors: population density, GDP, nighttime light.

Transportation location factors: distance to roads, distance to railways, distance to residential areas, distance to rivers, distance to landmarks and venues (Badaling, Horticultural Exhibition Park, Winter Olympics venues, etc.).

(2) Model Validation

Land use data from 2015 and 2020 were used to simulate 2025 land use. For the LEAS module, we adopted the default random forest settings [11]: random sampling with a sampling rate of 0.01, 20 decision trees, and mtry = 9 (two-thirds of the 13 driving factors). For the CARS module, the neighborhood size was set to the default value of 3. After multiple calibration trials, the patch generation threshold was set to 0.6, the expansion coefficient to 0.2, and the percentage of seeds to 0.1. The transition cost matrix was constructed based on the historical land use transitions observed from 2015 to 2020, combined with scenario-specific policy constraints as described in Scenario Settings. Future land demand for each scenario was calculated using the Markov Chain method based on the 2015–2025 transition probabilities, and the iteration number was set to 100. The simulation results were compared with actual 2025 data, and accuracy was verified using the Kappa coefficient and overall accuracy (OA).

(3) Scenario Settings

Natural development (ND): This scenario continues the land use change trend from 2015 to 2025 without additional policy interventions, with conversion restricted only for water areas (Figure 2). The transition matrix is presented in Table 3.

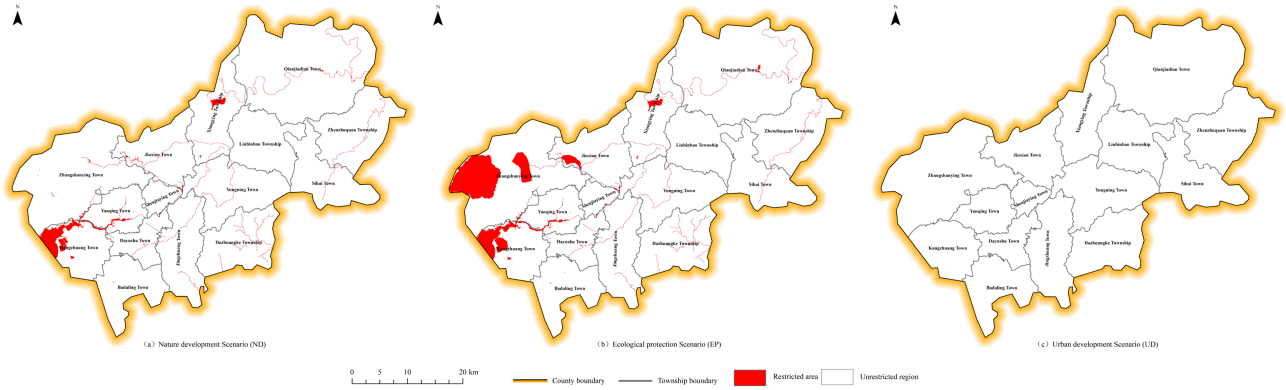

Figure 2. Distribution of restricted development areas under different development scenarios in 2035.

Table 3. Transition cost matrices for the ND scenarios.

2025\2035	Cropland	Forest	Grassland	Water	Construction Land
Cropland	1	1	1	1	1
Forest	1	1	1	1	1
Grassland	1	1	1	1	1
Water	1	1	0	1	1
Construction land	1	1	1	1	1

Ecological protection (EP): Based on the Yanqing District Master Plan (Territorial Spatial Planning) (2021–2035) [29] and the Regulations of Beijing Municipality on Ecological Protection and Green Development in Ecological Conservation Areas [30], ecological protection redlines and protected areas (Yeyahu Wetland, Songshan, etc.) were designated as restricted development zones (Figure 2). The probability of forest, grassland and water converting to construction land was reduced by 50% [19]. While the protected areas are mandated by policy [29,30], the 50% reduction is a modeling assumption based on literature precedents [19]. The transition matrix is presented in Table 4.

Table 4. Transition cost matrices for the EP scenarios.

2025\2035	Cropland	Forest	Grassland	Water	Construction Land
Cropland	1	1	0	0	0
Forest	1	1	1	0	0
Grassland	1	1	1	0	0
Water	1	1	1	1	1
Construction land	1	1	1	1	1

Urban development (UD): Based on the 14th Five-Year Plan for National Economic and Social Development of Yanqing District [31] and new urbanization targets, moderate expansion within urban development boundaries was permitted. The neighborhood weight of construction land was increased to 1.0 [19] (Table 5) to represent the highest expansion priority, consistent with urbanization targets [31] but selected as a modeling assumption rather than a policy mandate; restrictions on cropland and forest converting to construction

land were removed, and construction land was set as nonconvertible to other types. The transition matrix is presented in Table 6.

Table 5. Neighborhood weights for simulated scenarios.

Development Scenario	Cropland	Forest	Grassland	Water	Construction Land
Natural Development	0.2271	0.6317	0.1023	0.1351	0.2332
Ecological Protection	0.2271	0.6317	0.1023	0.1351	0.2332
Urban Development	0.2271	0.6317	0.1023	0.1351	1

Table 6. Transition cost matrices for the UD scenarios.

2025\2035	Cropland	Forest	Grassland	Water	Construction Land
Cropland	1	1	1	1	1
Forest	1	1	1	1	1
Grassland	1	1	1	1	1
Water	1	1	0	1	1
Construction land	0	0	0	0	1

It should be noted that the term "construction land reclamation" refers to the area of land classified as construction land in 2025 that converts to cropland by 2035 in the simulation. This is an emergent outcome of the PLUS model simulation, not a predefined policy parameter. Thus, the reclamation area varies across scenarios as a result of the different constraint settings, rather than being imposed as a fixed input value.

2.3.3. Sustainable Development Evaluation Framework

Based on the multi-scenario simulation results, the sustainability of different development pathways was comprehensively evaluated from multiple dimensions, including construction land expansion intensity, cropland protection effectiveness, and ecological land stability. Differentiated regulation recommendations were proposed accordingly [30,32].

3. Results and Analysis

3.1. Spatiotemporal Characteristics of Land Use Change

Based on land use data from 2015, 2020 and 2025 (Figure 3), the land use types in Yanqing District were classified into five categories—cropland, forest, grassland, water, and construction land—to reveal the spatiotemporal evolution characteristics of the land use pattern.

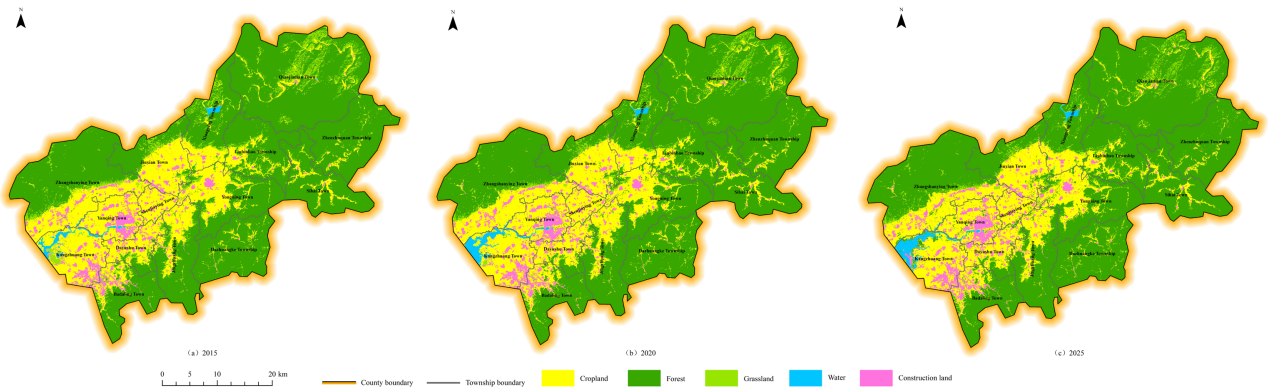

Figure 3. Land use types in Yanqing District from 2015 to 2025.

3.1.1. Land Use Area Changes

Based on land use data from 2015, 2020 and 2025 (Table 7), the total area of Yanqing District is 2009.44 km^2. The overall evolution is characterized by "forest dominance with sustained growth, rapid expansion of construction land, sharp contraction of grassland, steady decline of cropland, and significant increase in water area".

Table 7. Land use area changes in Yanqing District, 2015–2025.

Land Use Type	2015	2020	2025	2015–2020 Change	2020–2025 Change	2015–2025 Change
Cropland	490.56 (24.41%)	483.62 (24.07%)	465.20 (23.15%)	−6.94 (−1.41%)	−18.42 (−3.81%)	−25.36 (−5.17%)
Forest	1308.38 (65.11%)	1332.66 (66.32%)	1348.55 (67.11%)	+24.28 (+1.86%)	+15.89 (+1.19%)	+40.17 (+3.07%)
Grassland	104.84 (5.22%)	72.25 (3.60%)	66.61 (3.31%)	−32.59 (−31.09%)	−5.64 (−7.81%)	−38.23 (−36.47%)
Water	13.77 (0.69%)	20.99 (1.04%)	22.36 (1.11%)	+7.22 (+52.43%)	+1.37 (+6.53%)	+8.59 (+62.38%)
Construction land	91.89 (4.57%)	99.92 (4.97%)	106.72 (5.31%)	+8.03 (+8.74%)	+6.80 (+6.81%)	+14.83 (+16.14%)
Total	2009.44	2009.44	2009.44	-	-	-

Note: Total area is the area of Yanqing District, in km^2; values in parentheses are percentages of the district area.

Forest remained the dominant land type, increasing from 65.11% to 67.11%, with a cumulative increase of 40.17 km^2, closely aligning with Beijing's "Million-Mu Afforestation" project [33]. Grassland decreased sharply by 38.23 km^2 (−36.47%), indicating the continuous narrowing of "flexible ecological space" [27]. Cropland decreased by 25.36 km^2 (−5.17%), with an accelerating loss rate (the latter five years were 2.65 times the former five years). Construction land increased by 14.83 km^2 (+16.14%), with growth rates higher in the earlier period and lower in the later period, reflecting the phased differences between event preparation and post-event transition [26]. Water area showed the largest proportional increase (+62.38%, +8.59 km^2), mainly benefiting from river ecological water replenishment and the construction of artificial water bodies in the competition areas [34]. However, water area accounts for only 1.11% of the district, so its ecological leverage effect and post-event maintenance costs need to be weighed.

3.1.2. Land Use Transition Characteristics and Ecological Conversion Direction

In terms of spatial pattern, forest is concentrated in the western and northern mountainous areas, cropland is distributed in the Yanqing Basin and the southeastern plain, and construction land exhibits a "one core, multiple nodes" pattern (with Yanqing urban area as the core, and Kangzhuang, Badaling, and Yongning as secondary centers) [28]. Based on the transition matrices for the two periods (Tables 8 and 9), the Ecological Conversion Direction Index (*ECDI*) was further calculated to quantitatively characterize the nature of the transitions (Figure 4).

Table 8. Land use transition matrix, 2015–2020 (km^2).

2015\2020	Cropland	Forest	Grassland	Water	Construction Land	Total Outflow
Cropland	460.53	13.18	2.04	6.08	8.73	30.03
Forest	10.48	1294.71	2.8	0.03	0.36	13.67
Grassland	10.82	24.68	67.37	1.37	0.6	37.47
Water	0.64	0.02	0	13.09	0.02	0.68
Construction land	1.15	0.07	0.04	0.42	90.21	1.68
Total Inflow	23.09	37.95	4.88	7.9	9.71	-

Table 9. Land use transition matrix, 2020–2025 (km^2).

2020\2025	Cropland	Forest	Grassland	Water	Construction Land	Total Outflow
Cropland	440.380	24.710	4.070	3.030	11.430	43.24
Forest	12.500	1305.370	12.660	0.170	1.960	27.290
Grassland	4.270	17.610	49.480	0.420	0.470	22.770
Water	0.670	0.300	0.230	18.530	1.260	2.460
Construction land	7.380	0.560	0.170	0.210	91.600	8.320
Total Inflow	24.82	43.18	17.13	3.83	15.12	-

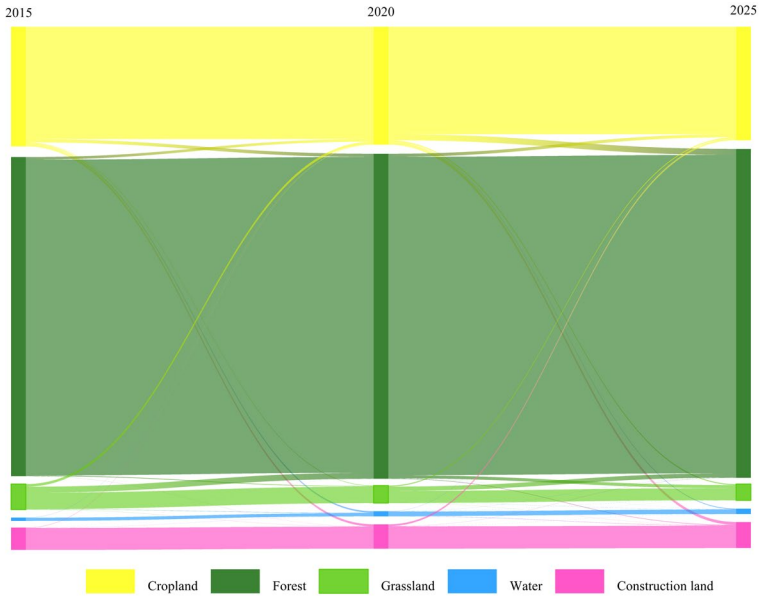

Figure 4. Land use transition Sankey diagram in Yanqing District, 2015–2025.

Comparison of the two periods reveals a phased shift in land management models. From 2015 to 2020, the total conversion area was 83.53 km^2, dominated by a "development-priority" pattern—cropland had a net outflow of 6.94 km^2 and grassland had a net outflow of 32.59 km^2, serving infrastructure development and ecological spatial restructuring [26]. From 2020 to 2025, the total conversion area surged to 104.08 km^2 (+24.6%). The most significant change was the large-scale "reverse conversion" of construction land—reclamation and ecological withdrawal totaled 8.32 km^2, 4.95 times that of the previous period. Meanwhile, the cropland to forest conversion reached 24.71 km^2 (+87.5%), forming a reciprocal conversion flow pattern of "cropland to forest" and "construction land to cropland" occurring in parallel. This marks the entry of Yanqing's land management into a refined governance stage characterized by "incremental control, stock remediation, and ecological expansion" [32,35].

The *ECDI* calculations show that the *ECDI* was 0.313 for 2015–2020 and 0.178 for 2020–2025. Both values are positive, indicating that ecological improvement remained the dominant direction, but the decline of 0.073 in the later period suggests a weakening after the events. This decline stems from the increase in reverse conversions of forest to grassland (12.66 km^2) and forest to cropland (12.50 km^2) in the later stage. This does not represent ecological degradation, but rather reflects structural vegetation adjustments after the Winter Olympics and the development of understory economy [26]. The bidirectional conversion pattern in the transition matrices—the forest–cropland competition (net inflow expanding from 2.70 km^2 to 12.21 km^2) and the construction land–cropland competition (net inflow narrowing from 7.58 km^2 to 4.05 km^2)—further indicates that land use change is

the result of dynamic interplay among policy regulation, economic drivers, and ecological demands [2,27].

3.2. Analysis of Driving Factors of Land Use Change

Based on the LEAS module, 13 driving factors (Figure 5) were selected, and the contribution rates of driving factors to the expansion of each land use type in the two periods were calculated separately (Figures 6 and 7) to reveal the structural transformation of the driving mechanisms. These contribution rates reflect predictive importance derived from the random forest algorithm embedded in the PLUS model's LEAS module, indicating statistical associations rather than causal relationships [11].

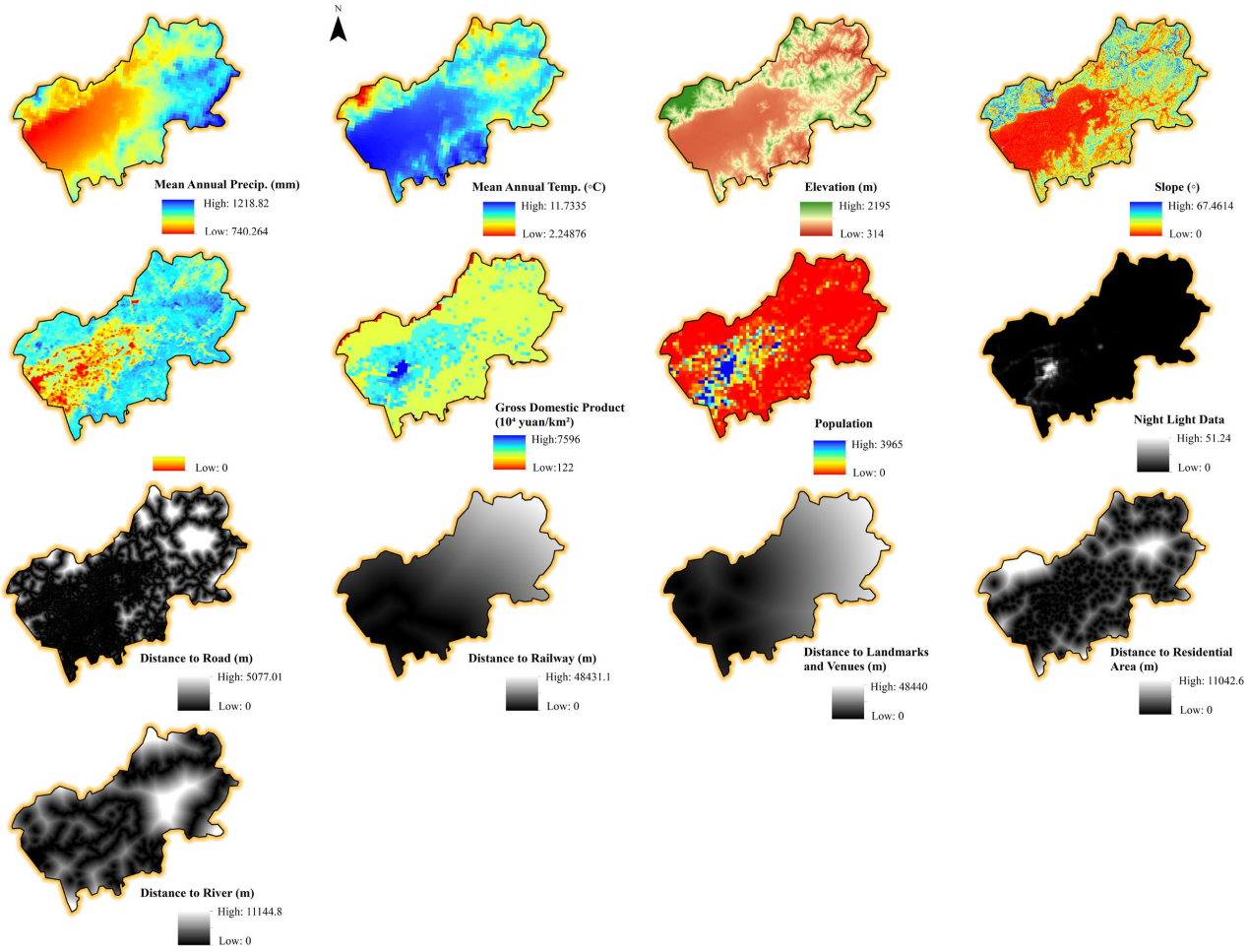

Figure 5. Spatial distribution of various influencing factors of Patch-generating Land Use Simulation (PLUS) in the study area.

The driving factors for construction land expansion underwent a fundamental restructuring. From 2015 to 2020, distance to residential areas (29.52%) and nighttime light (22.64%) were absolutely dominant, indicating that urban development followed an "outward expansion of built-up areas" model. From 2020 to 2025, distance to residential areas remained the top factor (26.25%), but the contribution of nighttime light dropped sharply by 90% (22.64% to 2.31%), while NDVI rose to 18.24% to become the second most important factor. New construction land increasingly shifted toward areas of lower vegetation cover, marking the entry of urban development into a new stage of "ecology-driven intensification". Notably, the contribution of distance to landmarks/venues ranked from 2.81% to 5.14%, indicating that major events had extremely limited direct spatial traction on

new construction land [36]. Development activities remained consistently concentrated in existing urban clusters such as Yanqing urban area and Kangzhuang Town.

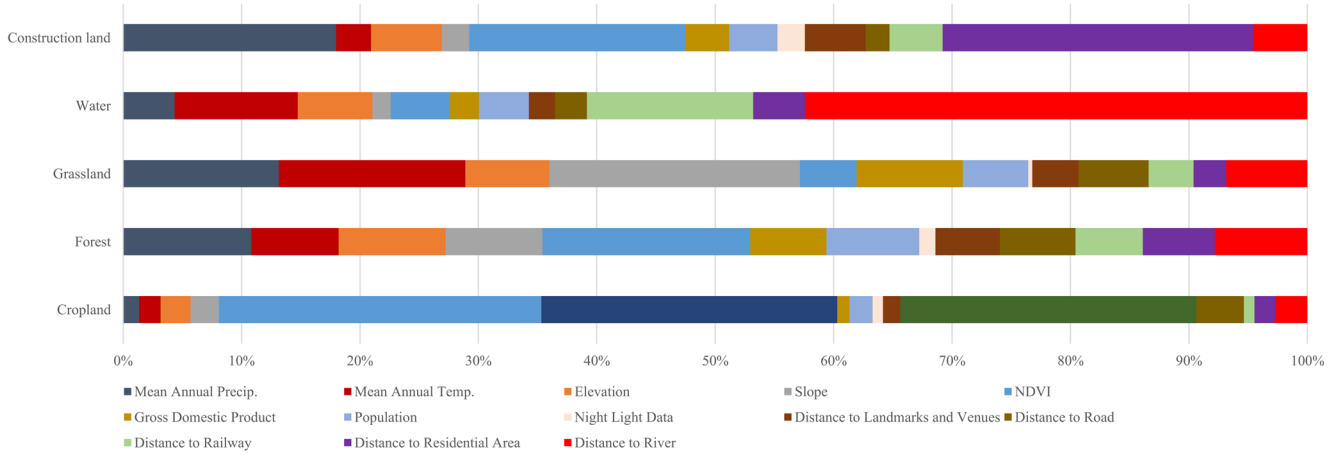

Figure 6. Contributions of driving factors from 2015 to 2020.

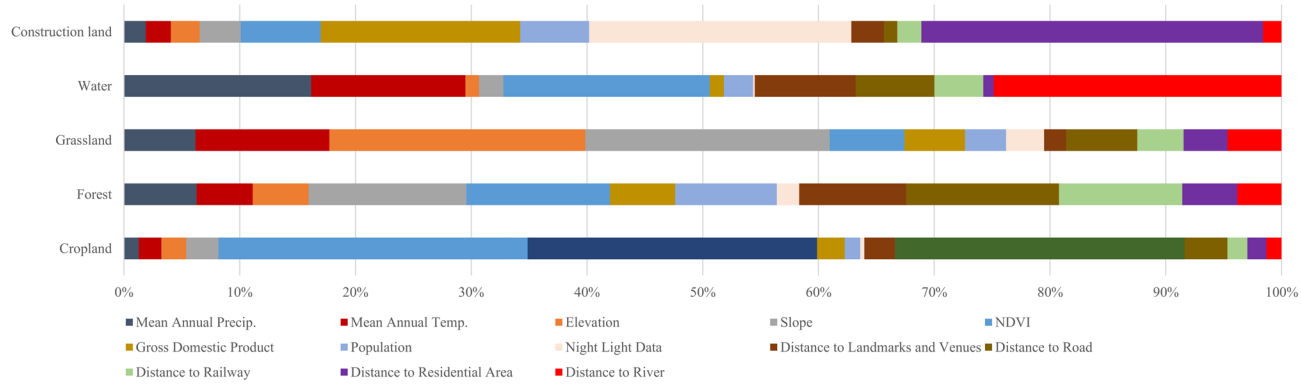

Figure 7. Contributions of driving factors from 2020 to 2025.

The dominant factors for cropland expansion shifted from a dual "location + event" drive (distance to roads 14.88%, slope 11.14%, distance to venues 10.63%) in the earlier period to a single "water–soil matching" drive (distance to roads 16.09%, distance to rivers 10.85%) in the later period. The reclamation effect of temporary land around venues faded [34], and cropland expansion returned to agricultural location logic centered on transportation convenience and water resource availability.

Forest expansion shifted comprehensively from "suitability-oriented" to "ecological quality-oriented". In the earlier period, slope (13.62%) and NDVI (12.41%) were dominant, with new forest planted in topographically suitable areas. In the later period, NDVI jumped to 17.55% to become the overwhelmingly dominant factor, indicating a strategy shift from "area expansion" to "quality-oriented enhancement"—prioritizing the replanting and closure of sparse forests and low-cover forests to enhance carbon sink capacity and ecological functions [33].

Grassland expansion shifted from "terrain-constrained" to "climate-responsive". In the earlier period, elevation (22.10%) and slope (21.11%) were dominant, with new grassland confined to steep mountainous areas in the west and north. In the later period, slope remained the top factor (21.16%), but mean annual temperature (15.74%) and precipitation (13.15%) rose to second and third place, with the combined contribution of climatic factors increasing by 11 percentage points. This is consistent with the observed vertical migration of vegetation belts at high altitudes under global warming [37].

The driving factors for water expansion became highly concentrated, with the contribution of distance to rivers surging from 24.86% to 42.43%. This directly corresponds to the spatial layout of the comprehensive ecological water replenishment and wetland restoration projects for the Guishui River and Caihe River during Yanqing's 14th Five-Year Plan period [34].

Overall, the driving mechanisms of land use in Yanqing exhibited marked changes: the contribution of distance to landmarks/venues decreased substantially for cropland, forest, grassland, and water after the events, with the largest declines exceeding 50%. This suggests that event traction may have a transient characteristic [36], and post-event development appears to rely on routine institutional arrangements. NDVI evolved from a factor that only explained forest expansion in the earlier period. In the later period, it became a dual key factor. It was negatively associated with constraining construction land expansion (18.24%) and positively associated with forest quality improvement (17.55%), suggesting a growing influence of ecological factors in the decision-making core of urban development and ecological construction. The shift in forest expansion from slope-dominance to NDVI-dominance and water expansion from multi-driver to single-river dominance together indicate that Yanqing's ecological construction has moved beyond the "area expansion" stage and entered a new cycle of "quality-oriented enhancement" [33,38].

3.3. Multi-Scenario Land Use Simulation (2035)

3.3.1. Model Accuracy Verification

Land use data from 2015 and 2020 were used to simulate 2025 land use, and the results were compared with actual 2025 data for validation (Figure 8). Based on the proportion of expansion areas of different land types and 2015–2020 calibration, the neighborhood weights for cropland, forest, grassland, water, and construction land were set to 0.2271, 0.6317, 0.1023, 0.1351, and 0.2332, respectively [7].

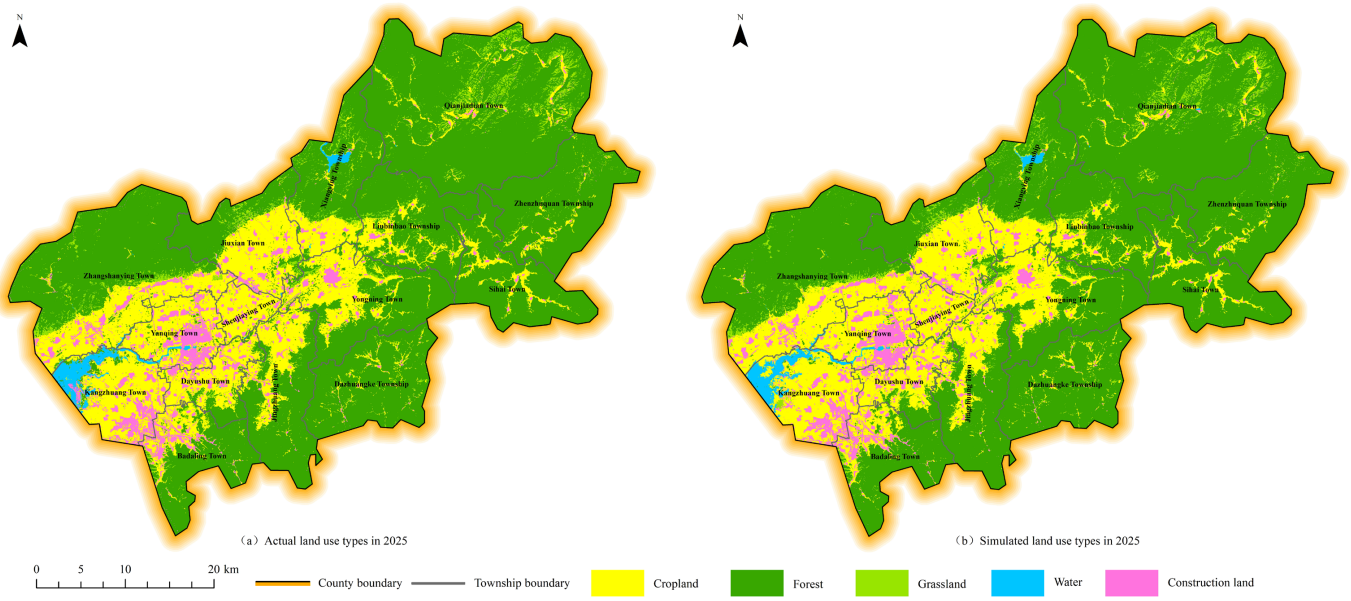

Figure 8. Actual and simulated distribution of different land use types in 2025 of the study area.

The calibrated parameters were then used to simulate the 2025 land use pattern as an independent validation, without further adjustment. The simulation results yielded a Kappa coefficient of 0.91 and an overall accuracy (OA) of 0.95, meeting the model accuracy requirements (Kappa > 0.75). This indicates that the PLUS model has good applicability in Yanqing District [11,17].

3.3.2. Multi-Scenario Land Use Simulation Results

Based on the land use change patterns from 2015 to 2025 and Yanqing's development plans, the land use patterns under the three scenarios for 2035 were simulated (Figure 9), and area statistics were obtained (Tables 10 and 11).

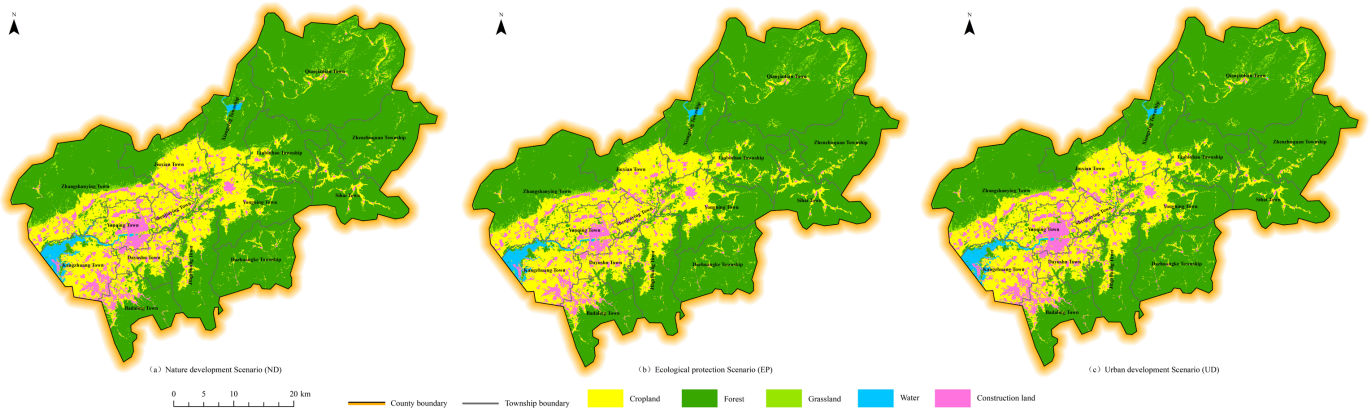

Figure 9. Spatial distribution of land use types under different future scenarios in 2035.

Table 10. Future land demand for each scenario calculated by Markov Chain (in pixels).

Scenario	Cropland	Forest	Grassland	Water	Construction Land	Total
2035 (ND)	482,591	1,538,501	60,928	27,128	124,596	2,233,744
2035 (EP)	482,590	1,539,003	61,089	28,002	123,060	2,233,744
2035 (UD)	477,783	1,537,801	60,765	26,877	130,518	2,233,744

Table 11. Area of various types under different scenarios in 2035 (km^2).

Land Use Type	2025	2035 (ND)	2035 (EP)	2035 (UD)
Cropland	465.2	435.27	449.24	429.97
Forest	1348.55	1388.13	1388.57	1387.47
Grassland	66.61	50.7	50.81	50.59
Water	22.36	23.51	22.15	24.19
Construction land	106.72	111.83	98.67	117.22

(1) Natural Development Scenario (ND)

Continuing the historical trend, construction land increased to 111.83 km^2 (+5.11 km^2, +4.8%), mainly from cropland conversion (12.23 km^2). Forest steadily increased to 1388.13 km^2 (+39.58 km^2), with increments mainly from cropland conversion to forest (26.86 km^2) and grassland afforestation (18.65 km^2), indicating the strong inertia of the "Million-Mu Afforestation" project [33]. Cropland decreased to 435.27 km^2 (−29.93 km^2, −6.4%). Notably, construction land reclamation to cropland reached 5.60 km^2, reflecting the rigid constraint of the "increase–decrease linkage" mechanism on construction land—even under natural development conditions, the effect of Beijing's reduction-oriented development framework on Yanqing remains significant [32,35].

(2) Ecological Protection Scenario (EP)

The EP scenario is the only pathway that achieves a net reduction in construction land (−8.05 km^2, −7.5%), decreasing to 98.67 km^2. This is highly consistent with the "reduction in urban and rural construction land" target proposed in the Beijing Urban Master Plan (2016–2035) [32]. Forest area reaches 1388.57 km^2 (+40.02 km^2), the highest among the three scenarios, with incremental structure dominated by cropland to forest (27.32 km^2)

and grassland to forest (18.58 km^2). Cropland is retained at 449.24 km^2 (−15.96 km^2, −3.4%), the smallest decline. The most prominent feature is the reclamation of construction land to cropland, reaching 11.02 km^2 (twice that of the ND scenario; these values are model-generated outcomes under each scenario's specific constraint settings, rather than externally imposed reclamation targets), forming a "spatial replacement" with cropland to construction land (4.54 km^2)—the EP scenario does not prohibit development, but rather concentrates limited construction indicators in areas with lower ecological sensitivity while achieving overall reduction through the orderly withdrawal of inefficient construction land within ecological redline areas [29]. This reciprocal conversion model is the core feature distinguishing the EP scenario from ND and UD.

(3) Urban Development Scenario (UD)

Construction land reaches 117.22 km^2 (+10.50 km^2, +9.8%), the highest among the three scenarios. Cropland declines sharply to 429.97 km^2 (−35.23 km^2, −7.6%), the lowest among the three scenarios. Forest area is 1387.47 km^2 (+38.92 km^2), with the smallest increase among the three scenarios. Notably, water area increases to 24.19 km^2 (+1.83 km^2) in the UD scenario, making it the only scenario with a significant increase in water area, reflecting the tendency toward artificial water body construction under urban development orientation [26].

3.3.3. Comparison of Land Use Transition Characteristics Under Multiple Scenarios

Figure 10 presents the chord diagrams of land use transitions from 2025 to 2035 under the three scenarios, visually reflecting the systematic differences in transition directions and scales among the scenarios.

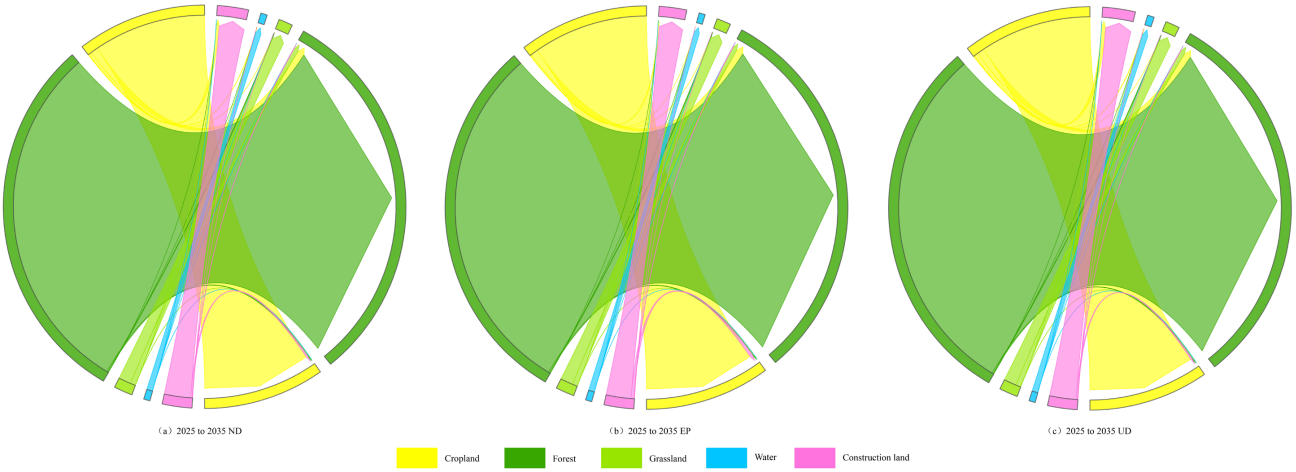

Figure 10. Chord diagram of land use transitions under multiple scenarios from 2025 to 2035.

The transition structure of the ND scenario is characterized by mutual conversion dynamics: cropland to forest (26.86 km^2) coexists with cropland to construction land (12.23 km^2), and construction land to cropland reclamation (5.60 km^2) together with grassland to forest (18.65 km^2) constitutes the main sources of net forest growth [35]. The EP scenario is centered on "spatial replacement + reduction and quality-oriented enhancement": construction land to cropland reclamation (11.02 km^2) is twice that of ND, and cropland to forest (27.32 km^2) further expands, achieving a dynamic balance between development and protection through the withdrawal of inefficient construction land and ecological expansion [29,30]. The UD scenario is characterized by "indirect replacement-dominated development": its development pathway is more complex—cropland to construction land (4.54 km^2) is not the largest source, but indirect conversions such as forest to cropland (4.42 km^2) and grassland to cropland (1.08 km^2) increase significantly, indicating that devel-

opment land indirectly occupies ecological space through multi-level replacement chains. The transition differences among the three scenarios indicate that the construction land reclamation rate is the core policy lever determining Yanqing's development pathway—the ND scenario maintains basic balance through 5.60 km^2 of reclamation, the EP scenario achieves reduction and quality improvement through 11.02 km^2 of reclamation, and the UD scenario, while maintaining the same reclamation scale as ND (4.83 km^2), releases more new development indicators, thereby supporting the largest increase in construction land.

3.4. Urban Sustainable Development Analysis Based on Simulation Results

To provide a structured sustainability assessment, we evaluate the three scenarios across three predefined dimensions—construction land control, cropland protection, and ecological security—each measured by a corresponding indicator: construction land area change, cropland retention rate, and ecological land ratio (forest + grassland + water). The scenarios were comprehensively evaluated from three dimensions—construction land control, cropland protection, and ecological security and carbon sink functions—and benchmarked against relevant plans and regulations [29,30,32]. In terms of construction land control, the UD scenario (117.22 km^2, +10.50 km^2) directly conflicts with Beijing's reduction-oriented development targets. Only the EP scenario achieves a net reduction to 98.67 km^2 (−7.5%), which is highly consistent with the "reduction of urban and rural construction land" target set in the Beijing Urban Master Plan [32]. In terms of cropland protection, the UD scenario reduces cropland sharply to 429.97 km^2 (−35.23 km^2), while the EP scenario retains 449.24 km^2 (−15.96 km^2), the smallest decline among all scenarios, which can better fulfill the permanent basic cropland protection target defined in the Yanqing District Master Plan (the cultivated land retention area shall be no less than 151.3 km^2, and the permanent basic cropland protection area shall be no less than 138.7 km^2) [29]. In terms of ecological security, the UD scenario has the smallest forest increase (+38.92 km^2) and more reverse conversions, while the EP scenario reaches 1388.57 km^2 (+40.02 km^2), with increments dominated by cropland to forest (27.32 km^2) and grassland to forest (18.58 km^2). Combined with the Million-Mu Afforestation project [33], the EP scenario is more conducive to the continued enhancement of ecosystem service value [39].

To provide a unified quantitative comparison of the three scenarios, we constructed a Composite Ecological Stability Index (*ESI*) as the decision rule for scenario ranking. The *ESI* is calculated as the normalized sum of ecological land ratio and cropland retention rate, minus the normalized construction land expansion intensity, with equal weights assigned to each component. This index captures the trade-offs among ecological protection, agricultural preservation, and urban expansion in a single value. Table 12 presents the *ESI* results for all three scenarios. The EP scenario achieves the highest cropland retention rate (96.56%), the lowest construction land expansion intensity (−7.55%), and the highest composite *ESI* (0.33). In contrast, the UD scenario exhibits the lowest cropland retention rate (92.43%), the highest construction land expansion intensity (+9.84%), and the lowest *ESI* (0.00). The ND scenario falls between the two, with an intermediate *ESI* of 0.19. These quantitative comparisons confirm that the EP scenario offers the most balanced pathway for harmonizing urban development with ecological conservation, while the UD scenario carries substantially higher anthropogenic pressure on the territory.

It should be noted that the three scenarios have nearly identical ecological land ratios (72.73–72.77%), so the *ESI* differences are primarily driven by cropland retention and construction land expansion rather than ecological land ratio. The *ESI* ranking reflects scenario preferences under the adopted analytical assumptions rather than an objective optimum. The ecological land ratio is retained in the index because it represents an

important policy dimension conceptually, although it has limited empirical differentiating power in this specific case.

Table 12. Unified assessment of land use scenarios using composite indicators.

Indicator	ND Scenario	EP Scenario	UD Scenario
Raw values			
Ecological land ratio (forest + grassland + water, %)	72.77%	72.73%	72.77%
Construction land expansion intensity (%)	+4.79%	−7.55%	+9.84%
Cropland retention rate (%)	93.56%	96.56%	92.43%
Normalized values (Min-Max, [0, 1])			
Ecological land ratio (normalized)	1.00	0.00	1.00
Construction land expansion (normalized)	0.71	0.00	1.00
Cropland retention (normalized)	0.27	1.00	0.00
Composite Ecological Stability Index (*ESI*)	0.19	0.33	0.00
Ranking	2	1	3

Note: ESI = (EcoNorm × w_1 + CropNorm × w_2 − ConstrNorm × w_3)/(w_1 + w_2 + w_3), where w_1, w_2, and w_3 are the weights for ecological land ratio, cropland retention, and construction land expansion, respectively. Under the equal-weight baseline, $w_1 = w_2 = w_3 = 1$, yielding ESI = (EcoNorm + FarmNorm − ConstrNorm)/3. Each indicator is normalized to the [0, 1] range using Min-Max normalization.

To assess the sensitivity of the *ESI* ranking to the equal-weight assumption, we conducted additional analyses using four alternative weighting schemes, varying the relative importance assigned to ecological land ratio, cropland retention, and construction land expansion. Table 13 presents the results.

Table 13. Sensitivity analysis of *ESI* rankings under different weighting schemes.

Weighting Scheme			ND	EP	UD	Ranking
Ecological Land Ratio	**Construction Land Expansion Intensity**	**Cropland Retention Rate**				
1	1	1	0.187	0.333	0.000	EP > ND > UD
1	0.5	0.5	0.366	0.4	0.2	EP > ND > UD
1	1	0.5	0.17	0.2	0	EP > ND > UD
0.5	1	1	0.024	0.4	−0.2	EP > ND > UD
0.5	0.5	1	0.208	0.5	0	EP > ND > UD
	Ranking		2	1	3	

Under all five weighting schemes (including the equal-weight baseline), EP consistently ranks highest, ND second, and UD lowest. While the absolute *ESI* values differ across schemes, the relative scenario ranking is stable. This confirms that the preference for EP as the most balanced scenario is robust to reasonable variations in weight assignments. However, it must be emphasized that this conclusion is conditional on the analytical assumptions adopted in this study—specifically, the three-dimensional evaluation framework, the Min-Max normalization, and the set of alternative weighting schemes tested. The *ESI* ranking should therefore be interpreted as a scenario preference under these assumptions, rather than an objective or universally applicable optimum. For Yanqing District, EP emerges as the preferred pathway for sustainable urban development under the given analytical framework.

Based on the multi-dimensional assessment, the EP scenario emerges as the preferred pathway under the adopted analytical assumptions for Yanqing District to achieve the dual goals of "ecological conservation area" positioning and "post-event sustainable development"—maintaining moderate urban development (98.67 km^2 of construction land)

while securing the ecological safety bottom line (1388.57 km^2 of forest) and the cropland redline (449.24 km^2). This is fully consistent with the principle of "prioritizing ecology, systematic governance, and green development" set forth in the Regulations of Beijing Municipality on Ecological Protection and Green Development in Ecological Conservation Areas [30]. The UD scenario has the lowest *ESI*, indicating that its development pattern is incompatible with the strategic requirements of the capital's ecological barrier [27]. It is recommended that Yanqing District strictly implement the "three zones and three lines" control system in territorial spatial planning [29], adopt the EP scenario as a guide, and pursue a development path of "reduction, quality improvement, and ecological priority".

4. Discussion

4.1. Phased Impacts of Mega-Events on Land Use

This study finds that from 2015 to 2020 (the Horticultural Exhibition and Winter Olympics preparation period), the average annual growth rate of construction land reached 1.61 km^2/year, significantly higher than the 1.36 km^2/year from 2020 to 2025. The contribution of "distance to landmarks/venues" to the expansion of cropland, forest, and water was significant (10.63%, 9.22%, and 8.72%, respectively), suggesting that mega-events are associated with a notable short-term influence on land use change [31,36]. However, this direct traction effect rapidly faded in the post-event period—the contribution of distance to landmarks/venues showed marked declines for cropland, forest, grassland, and water, though its contribution to construction land increased slightly, replaced by the constraint of NDVI (18.24%) on construction land expansion and the return of nighttime light to conventional economic drivers. This suggests that the impact of mega-events may not be a simple linear process of "hosting-decline", but rather appears to follow a three-stage temporal sequence: rapid development during preparation—control during the event—transition and utilization after the event [36,40]. Yanqing's post-event transformation through the Horticultural Exhibition Park and sustainable utilization of Winter Olympics venues offers a potential reference for post-event sustainable development of host cities [41]. Similar patterns have been observed in areas such as Beijing's Olympic Forest Park and Guangzhou's Asian Games Town [36,40]. However, we acknowledge that other factors—such as concurrent socioeconomic policies, regional development strategies, and broader urbanization trends—may also have contributed to the observed changes.

It is worth noting that Yanqing's land use evolution from 2015 to 2025 can be summarized as a four-stage coupled process of "ecological expansion—event-driven—post-event restoration—orderly growth" [27,31]. Unlike the "construction land eroding ecological space" model found in developed eastern counties [42], or the post-Olympic urban sprawl observed in London (2012) and Rio (2016) [43], Yanqing, relying on the policy positioning of the ecological conservation area and the "window effect" of major events, achieved sustained net growth of forest (+40.17 km^2) and a consistently positive *ECDI* throughout the entire period while advancing urbanization. This demonstrates that under the combined action of strong ecological control policies and major ecological engineering projects, "urbanization" and "ecologization" are not a zero-sum game; rather, it is possible to achieve the synergistic pathway of "protecting while developing, developing while protecting" [38,42]. However, new issues—the narrowing of grassland reserve space (−38.23 km^2), the accelerating trend of cropland loss (−18.42 km^2 in the latter five years), and the maintenance costs of post-event artificial landscapes—also pose new governance challenges for Yanqing's next-stage sustainable development.

4.2. Methodological Contribution and Applicability of the Ecological Conversion Direction Index (ECDI)

This study innovatively constructs the Ecological Conversion Direction Index (*ECDI*), providing a concise and interpretable metric for characterizing the direction of regional ecological quality change. Unlike the traditional Ecological Quality Index (*EQI*), which focuses on static valuation [38,42], the *ECDI* focuses on the dynamic directionality of conversions—by distinguishing between "conversions to higher ecological value land types" (S_{eco_up}), and "reverse conversions" (S_{eco_down}), and normalizing by the total conversion area, it intuitively reflects the net direction of regional ecological succession. The *ECDI* calculations for the two periods in Yanqing show that the *ECDI* was 0.313 for 2015–2020 and 0.178 for 2020–2025. Although both remain positive, the decline of 0.073 in the latter period precisely captures the weakening effect of post-event forest reverse conversions (forest to grassland 12.66 km^2, forest to cropland 12.50 km^2) on the momentum of ecological improvement [26]—a structural information that is difficult to detect through simple area statistics alone. The advantages of the *ECDI* are: (1) simple calculation, requiring only the transition matrix; (2) clear directionality, with positive and negative values directly corresponding to ecological improvement/degradation; and (3) strong comparability, with normalization allowing comparison across different regions and time periods. This method can be extended to similar studies on the ecological effects of land use change, serving as a useful complement to the traditional *EQI* and ecological contribution rate.

4.3. Applicability and Methodological Advantages of the PLUS Model in Ecological Conservation Areas

The core value of the PLUS model in this Yanqing study lies in the matching of its algorithmic mechanisms with the complex land use changes in the ecological conservation area. Land use conversion rules in Yanqing are non-stationary over time (with significant differences in driving mechanisms between the event-preparation and post-event restoration periods) [36], and traditional models relying on fixed transition probabilities struggle to capture such phased mutations [8]. The LEAS module of PLUS employs random forest training independently for each period, adaptively identifying the dominant factor structures of different periods in terms of predictive importance (such as the role switch of NDVI from a forest explanatory factor to a constraint on construction land), avoiding dependence on static averages over the entire period [11,17]. This issue has also been noted in European land system studies [44]. At the same time, the spatial heterogeneity of the mountain–plain transition zone in Yanqing is extremely strong [45], and the same factor has vastly different constraint effects on mountain forest versus plain construction land. PLUS allows each land type to have its own independent expansion rule function [11,16], avoiding the spatial bias caused by unified regression coefficients [7,9]. At the patch scale, the multi-scenario simulation in Yanqing involves extensive two-way replacement between construction land and cropland, as well as forest edge restoration [20,28]. The multi-type random seed competition mechanism of PLUS can reproduce these discrete conversion processes through local evolution rules such as patch generation, disappearance, and merging [11,19]. The simulation results have greater spatial credibility at the local scale than traditional cellular automata [18], providing more refined spatial guidance for subsequent zoning control and site-level ecological restoration.

4.4. Policy Implications for Sustainable Urban Development

Our multi-scenario simulation results offer actionable policy insights for promoting sustainable urban transition in ecological conservation areas. First, the identification of the construction land reclamation rate as a core policy lever directly supports SDG 11.3 (inclusive and sustainable urbanization) by enabling compact urban growth without com-

promising ecological integrity [23,24]. Second, the superior performance of the EP scenario in maintaining forest cover and cropland stability contributes to SDG 15.1 (conservation of terrestrial ecosystems) [23,24], while the quantified trade-off between reclamation rates and urban expansion provides a measurable basis for spatial planning decisions. Importantly, the finding that the "pulse effect" of mega-events is transitory suggests that post-event spatial planning should shift from crisis-driven interventions to anticipatory governance—an insight that may be applicable to other cities hosting large-scale events in developing countries. Similar post-event planning challenges have been documented in studies of the London 2012 Olympics and the PyeongChang 2018 Winter Olympics [43,46]. Third, the *ECDI* offers a replicable metric for tracking ecological transition direction, which could be incorporated into local SDG monitoring frameworks.

These findings collectively suggest that sustainable urban transition in ecological conservation areas requires a shift from reactive to proactive governance—prioritizing the reclamation rate as a primary planning benchmark and embedding it within statutory territorial spatial planning. For Yanqing, this means adopting the EP scenario as a baseline for future urban master plan revisions.

4.5. Limitations and Future Research Directions

This study has several limitations. First, it does not fully consider the long-term impacts of climate change (such as temperature and precipitation changes) on the distribution of forest and grassland—although this study found that the combined contribution of climatic factors to grassland expansion increased by 11 percentage points in the later period, the driving factor settings of the PLUS model remain predominantly based on static historical trends. Second, it does not quantitatively assess ecosystem service values or carbon storage—as the capital's ecological barrier, Yanqing's carbon sink function and water conservation value are of critical importance, and future research could integrate the InVEST model for multi-dimensional trade-off analysis. Third, this study uses 2025 as the base year to project to 2035; future research could extend the simulation period to 2050 to examine longer-term land use evolution trends. Fourth, the long-term impacts of venue utilization on land use require continuous monitoring—the post-event transformation of the Horticultural Exhibition Park and Winter Olympics venues is still in the exploratory stage, and their spatial effects need to be verified through longer time series.

5. Conclusions

This study takes Yanqing District, Beijing, as the research object. Based on land use data from 2015, 2020 and 2025, it constructs a driving factor index system, employs the PLUS model to simulate land use patterns under three development scenarios for 2035, and evaluates the impacts of different scenarios on urban sustainable development. The main conclusions are as follows:

(1) A land use model of synergistic "ecological expansion" and "urbanization" is revealed. From 2015 to 2025, forest and construction land grew simultaneously, with grassland mainly converting to forest. The positive *ECDI* values (0.313 to 0.178) indicate that the net direction of land conversion remained ecologically positive throughout the period. This differs from the "construction land eroding ecological space" trajectory found in eastern counties, demonstrating that ecological conservation areas can pursue a path of coordinated protection and development.

(2) The Ecological Conversion Direction Index (*ECDI*) is constructed and demonstrates good applicability and interpretability. By characterizing the net direction of ecological quality evolution, the *ECDI* overcomes the limitations of traditional area statistics. The *ECDI* values for both periods in Yanqing are positive (0.313 to 0.178), indicating that

ecological improvement remained dominant throughout, though somewhat weakened after the events. This provides a quantitative basis for precisely adjusting ecological restoration policies.

(3) Marked changes in the driving mechanism were observed, suggesting a trend of transition from "event-response" toward "ecological constraint" is identified. Major event traction may have a transient characteristic, and post-event development momentum appears to require a return to routine institutional arrangements. Ecological logic has become increasingly influential in urban development decision-making, and ecological construction showed signs of transition from "area expansion" to a new cycle of "quality-oriented enhancement".

(4) Multi-scenario simulations clarify the optimal development pathway for Yanqing's future. The EP scenario is the only pathway fully consistent with Beijing's reduction-oriented development targets and the requirements of the ecological conservation area regulations—maintaining moderate development while securing the ecological safety baseline and the cropland redline, aligning with the requirements of SDG 11 (Sustainable Cities and Communities) and SDG 15 (Life on Land).

(5) The construction land reclamation rate is identified as the core policy variable determining the development pathway. The EP scenario achieves reduction and quality improvement through 11.02 km^2 of reclamation, while the UD scenario, although maintaining 4.83 km^2 of reclamation, releases more new development indicators. It is recommended that Yanqing adopt the EP scenario as a guide, institutionalizing reclamation rate as a statutory benchmark, enforcing urban growth boundaries, and operationalizing ecological redlines through adaptive monitoring.

Author Contributions: Conceptualization, M.L. and X.L.; methodology, E.Z., M.L., X.W. and Y.Z.; validation, X.L.; formal analysis, E.Z.; investigation, M.L.; resources, X.L. and J.B.; data curation, E.Z., M.L., X.W. and Y.Z.; writing—original draft preparation, E.Z.; writing—review and editing, M.L.; visualization, E.Z.; supervision, X.L.; project administration, E.Z. and M.L.; funding acquisition, X.L. and J.B.; X.L. and J.B. are both corresponding authors. All authors have read and agreed to the published version of the manuscript.

Funding: This research was funded by Geological survey projects, grant number DD202602110004.

Institutional Review Board Statement: Not applicable.

Informed Consent Statement: Not applicable.

Data Availability Statement: The datasets generated during and/or analyzed during the current study are available from the corresponding author on reasonable request.

Conflicts of Interest: The authors declare no conflicts of interest.

Abbreviations

The following abbreviations are used in this manuscript:

PLUS	Patch-generating Land Use Simulation
ECDI	Ecological Conversion Direction Index
LEAS	Land Expansion Analysis Strategy
CARS	Cellular Automata based on multi-type Random Seeds
SDGs	Sustainable Development Goals
NDVI	Normalized Difference Vegetation Index
ND	Natural development
EP	Ecological protection
UD	Urban development
OA	Overall Accuracy coefficient

LUCC	Land Use/Cover Change
InVEST	Integrated Valuation of Ecosystem Services and Trade-offs
GDP	Gross Domestic Product

References

1. Li, Q.; Wang, C.J.; Feng, T.; Du, C.J.; Zhang, B.L. Multi-scenario prediction of land use change and carbon storage in Shaanxi province based on the SD-PLUS coupled model. *J. Soil Water Conserv.* **2024**, *38*, 195–206. [CrossRef]
2. Yue, N.N.; Zhao, S.J.; Chai, L.N.; Li, X.Y.; Liu, S.M. Land Use/Land Cover Classification of the Qinghai Lake Basin Using Multitemporal Sentinel-1/2 Imagery. *Remote Sens.* **2026**, *18*, 2353. [CrossRef]
3. Wei, C.J.; Meng, J.J. Ecological Sensitivity Assessment and Spatial Pattern Analysis of Land Resources in China. *Acta Sci. Nat. Univ. Pekin.* **2022**, *58*, 157–168. [CrossRef]
4. Yang, H.X.; He, H.; Liu, B.; Yang, C.H.; Han, D.S. Multi-scenario Simulation of Land Use and Carbon Storage Assessment in Arid Region of Northwest China Based on the PLUS-InVEST-Geodetector Model. *Environ. Sci.* **2026**, *47*, 3049–3060. [CrossRef] [PubMed]
5. Wei, J.; Yue, W.; Li, M.; Liu, Y.; Song, Y. Multi-scenario urban growth boundaries and trade-offs among land use functions. *CITIES* **2025**, *159*, 105752. [CrossRef]
6. Li, Y.Z.; Feng, Z.Z.; Li, L.; Yang, X.Y.; Liu, M.; Wang, W.J. Evaluation of ecological sensitivity of terrestrial ecosystem in China. *Ecol. Sci.* **2024**, *43*, 129–139. [CrossRef]
7. Wang, B.S.; Liao, J.F.; Zhu, W.; Qiu, Q.Y.; Wang, L.; Tang, L.N. The weight of neighborhood setting of the FLUS model based on a historical scenario, A case study of land use simulation of urban agglomeration of the Golden Triangle of Southern Fujian in 2030. *Acta Ecol. Sin.* **2019**, *39*, 4284–4298. [CrossRef]
8. Xie, L.L.; Xu, J.L.; Zang, J.M.; Huang, T.N. Simulation and Prediction of Land Use Change in Guangxi Based on Markov-FLUS Model. *Res. Soil Water Conserv.* **2022**, *29*, 249–254. [CrossRef]
9. Li, Y.J.; Ye, C.S.; Huang, X.L. Temporal-Spatial Evolution and Scenario Simulation of Production-Living- Ecological Space in Nanchang Based on CLUE-S Model. *Res. Soil Water Conserv.* **2021**, *28*, 325–332. [CrossRef]
10. Ji, X.J.; Cheng, W.S. Simulation and Prediction of Land Use Change Based on CLUE-S and Markov Models. *Territ. Nat. Resour. Study* **2024**, *6*, 17–21. [CrossRef]
11. Liang, X.; Guan, Q.; Clarke, K.C.; Liu, S.; Wang, B.; Yao, Y. Understanding the drivers of sustainable land expansion using a patch-generating land use simulation (PLUS) model, A case study in Wuhan, China. *Comput. Environ. Urban Syst.* **2021**, *85*, 101569. [CrossRef]
12. Li, C.; Wu, Y.M.; Gao, B.P.; Zheng, K.J.; Wu, Y.; Li, C. Multi-scenario simulation of ecosystem service value for optimization of land use in the Sichuan-Yunnan ecological barrier, China. *Ecol. Indic.* **2021**, *132*, 108328. [CrossRef]
13. Zhao, B.; Li, S.; Liu, Z. Multi-Scenario Simulation and Prediction of Regional Habitat Quality Based on a System Dynamic and Patch-Generating Land-Use Simulation Coupling Model—A Case Study of Jilin Province. *Sustainability* **2022**, *14*, 5303. [CrossRef]
14. Zhang, Z.; Li, X.; Du, S.; Liu, C.; Shi, Z.; Yan, C. Spatial-temporal evolution analysis of multi-scenario land use and ecosystem services base on PLUS-Invest model, A case study in Beijing-Tianjin-Hebei region, China. *Sustain. Futures* **2025**, *10*, 101154. [CrossRef]
15. Zhang, P.; Li, Y.; Yin, H.; Chen, Q.; Dong, Q.; Zhu, L. Spatio-temporal variation and dynamic simulation of ecosystem carbon storage in the north-south transitional zone of China. *J. Nat. Resour.* **2022**, *37*, 1183. [CrossRef]
16. Zhao, H.H.; Liu, J.C.; Guo, Y.J.; Wang, H.M.; Gong, Z. Assessing the ecological sensitivity of the Northern Foothills of Qinling Mountains using DPSIRM and PLUS models. *Trans. Chin. Soc. Agric. Eng.* **2024**, *40*, 244–252. [CrossRef]
17. Xu, L.; Liu, X.; Tong, D.; Liu, Z.; Yin, L.; Zheng, W. Forecasting Urban Land Use Change Based on Cellular Automata and the PLUS Model. *Land* **2022**, *11*, 652. [CrossRef]
18. Yang, S.; Su, H.; Zhao, G.P. Multi-scenario simulation of urban ecosystem service value based on PLUS model, A case study of Hanzhong city. *J. Arid. Land Resour. Environ.* **2022**, *36*, 86–95. [CrossRef]
19. Li, C.; Gao, B.P.; Wu, Y.M.; Zheng, K.J.; Wu, Y. Dynamic simulation of landscape ecological risk in mountain towns based on PLUS model. *J. Zhejiang A F Univ.* **2022**, *39*, 84–94. [CrossRef]
20. Wang, X.; Wang, C.Y.; Lyu, F.N.; Cheng, S.L.; Yu, Z.R. Temporal and spatial variations of carbon storage and carbon sink improvement strategy at the dis trict and county level Based on PLUS InVEST model, Taking Yanqing District as an example. *Chin. J. Appl. Ecol.* **2023**, *34*, 3373–3384. [CrossRef] [PubMed]
21. Tang, J.T.; Yuan, J.; Wei, X.T.; Li, X.Y.; Sun, Z.T. Multi-scenario simulation of land use and carbon stock assessment in southern foothills of Qilian Mountains based on the PLUS-InVEST model. *Res. Soil Water Conserv.* **2026**, *33*, 264–273. [CrossRef]
22. Xu, R.M.; Wang, M.C.; Wang, F.Y.; Wei, L. Using coupled PLUS--InVEST model simulate and predict carbon storage changes under land use evolution in Heilongjiang watershed. *World Geol.* **2026**, *45*, 128–141.

23. UN General Assembly. *Work of the Statistical Commission Pertaining to the 2030 Agenda for Sustainable Development*; UN General Assembly: New York, NY, USA, 2017; Available online: https://undocs.org/A/RES/71/313 (accessed on 23 May 2026).
24. UN-Habitat. *World Cities Report 2020, The Value of Sustainable Urbanization, Technical Report*; United Nations Human Settlements Programme (UN-Habitat): Nairobi, Kenya, 2020.
25. Mata, R.; Izaurieta, F.; Quinzacara, C.; Correa, C.; Bustamante, G.; Nuñez, E.; Lobos-Calquin, D. Governing Vertical Urbanism, Property Rights, 3D Land Administration and the Sustainability of Inter-Building Connectivity. *Sustainability* **2026**, *18*, 7696. [CrossRef]
26. Guo, X.Y.; Yu, Y.; Hou, Q.M. Life cycle-based ecological quality assessment of Yanqing competition area of Beijing Winter Olympics based on GEE. *Beijing Surv. Mapp.* **2025**, *39*, 1251–1260. [CrossRef]
27. Zhang, G.X.; Ma, G.P.; Li, F.F.; Chen, X.L.; Zeng, J.W. Two-Decade Evolution and Prospect of Beijing Ecological Conservation Area Construction. *J. Ecol. Rural Environ.* **2025**, *41*, 160–171. [CrossRef]
28. Du, X.Y.; Lyu, F.N.; Wang, C.Y.; Yu, Z.R. Construction of ecological network based on MSPA-Conefor-MCR at the county scale, A case study in Yanqing District, Beijing China. *Chin. J. Appl. Ecol.* **2023**, *34*, 1073–1082. [CrossRef] [PubMed]
29. Yanqing District People's Government of Beijing Municipality. Yanqing District Master Plan (Territorial Spatial Planning) (2017–2035). 5 December 2019. Available online: http://www.bjyq.gov.cn/yanqing/zwgk/ghjh/zxgh/2959101/2957683/index.shtml (accessed on 1 July 2026).
30. The Standing Committee of Beijing Municipal People's Congress. Regulations of Beijing Municipality on Ecological Protection and Green Development in Ecological Conservation Areas. 21 April 2021. Available online: https://www.bjrd.gov.cn/xwzx/cwhgg/202104/t20210421_2364904.html (accessed on 1 July 2026).
31. Yanqing District People's Government of Beijing Municipality. The 14th Five-Year Plan for National Economic and Social Development of Yanqing District. 24 May 2021. Available online: http://www.bjyq.gov.cn/yanqing/ztlm95/2889786/2893069/index.shtml (accessed on 1 July 2026).
32. The People's Government of Beijing Municipality. Beijing Urban Master Plan (2016–2035). 29 September 2017. Available online: https://www.beijing.gov.cn/gongkai/guihua/wngh/csztgh/201907/t20190701_100008.html (accessed on 1 July 2026).
33. Beijing Municipal Forestry and Parks Bureau. 2022 Annual Construction Master Plan of Beijing's New Round of Million-Mu Afforestation and Greening Action Plan. 7 December 2021. Available online: https://yllhj.beijing.gov.cn/zwgk/zwxx/202112/t20211209_2557443.shtml (accessed on 1 July 2026).
34. Yanqing District People's Government of Beijing Municipality. The 14th Five-Year Water Development Plan of Yanqing District (2021–2025). 12 December 2021. Available online: http://www.bjyq.gov.cn/yanqing/zwgk/zcwj91/yq23271031/index.shtml (accessed on 1 July 2026).
35. Yanqing District People's Government of Beijing Municipality. The 14th Five-Year Plan for Land Resources Protection and Utilization of Yanqing District (2021–2025). 3 December 2021. Available online: https://fgw.beijing.gov.cn/fgwzwgk/2024zcwj/ghjhwb/wngh/202208/t20220824_3732852.htm (accessed on 1 July 2026).
36. Fan, J.; Li, Y.; Zhu, W.; Chen, Y.; Li, Y.; Hou, H.; Hu, T.G. Evaluating the Impact of Mega-Sports Events on Urbanization Focusing on Land-Use Changes Using a Scenario-Based Model. *Sustainability* **2021**, *13*, 1649. [CrossRef]
37. China Meteorological Administration. China Climate Change Blue Book (2023). 10 July 2023. Available online: https://www.cma.gov.cn/2011xwzx/2011xmtjj/202307/t20230710_5637531.html (accessed on 1 July 2026).
38. Wan, L.T.; Liu, X.D.; Guo, H.Q.; Xue, W.L.; Liu, K.X.; Li, L.; Wang, L.L. Spatio-temporal succession and prediction of carbon storage in ecological conservation area of western Beijing based on InVEST-PLUS model. *Geol. Bull. China* **2025**, *44*, 1272−1284. [CrossRef]
39. Zhang, Q.; Huang, R.; Zhu, C.; Huang, L.; Yang, D. Integrating land use simulation and carbon assessment for sustainable urban planning in Fuzhou metropolitan area using PLUS and InVEST models. *Sci. Rep.* **2025**, *15*, 30382. [CrossRef] [PubMed]
40. Peng, T.; Yan, Y.T. Influence of Stadiums and Gymnasiums for Major Sports Competitions to Urban Space Development, Guangzhou Asian Games Town Example. *Planners* **2011**, *27*, 10–14.
41. Yanqing District People's Government of Beijing Municipality. The 14th Five-Year Plan for Ecological Environmental Protection of Yanqing District. 21 January 2022. Available online: http://www.bjyq.gov.cn/yanqing/zwgk/zcwj91/yq23280227/index.shtml (accessed on 1 July 2026).
42. Yao, L.L.; Ma, J.; Li, Y.J.; Li, K.M. Study on Beijing Land Utilization Change and Its Ecological Environmental Effect. *Hunan Agric. Sci.* **2021**, *8*, 91–94. [CrossRef]
43. Baroghi, F.; Ribeiro, P.J.G.; Fonseca, F. Towards a Holistic Framework for the Olympic-Led Sustainable Urban Planning Process. *Sustainability* **2024**, *16*, 951. [CrossRef]
44. Verburg, P.H.; Crossman, N.; Ellis, E.C.; Heinimann, A.; Hostert, P.; Mertz, O.; Nagendra, H.; Sikor, T.; Erb, K.H.; Golubiewski, N. Land system science and sustainable development of the earth system, A global land project perspective. *Anthropocene* **2015**, *12*, 29–41. [CrossRef]

45. Yang, Y.Y.; Yang, M.Y.; Wang, W.Y.; Chen, H.; Sun, X. Spatial heterogeneity and driving factors of ecosystem service trade-offs in Beijing's ecological conservation area, Insights for spatial planning and management. *Landsc. Ecol.* **2025**, *41*, 19. [CrossRef]
46. Do, J.W.; Ahn, S.H.; Kang, J.Y. Urbanization effect of mega sporting events using sentinel-2 satellite images, The case of the Pyeongchang Olympics. *Sustain. Cities Soc.* **2021**, *74*, 103158. [CrossRef]

Disclaimer/Publisher's Note: The statements, opinions and data contained in all publications are solely those of the individual author(s) and contributor(s) and not of MDPI and/or the editor(s). MDPI and/or the editor(s) disclaim responsibility for any injury to people or property resulting from any ideas, methods, instructions or products referred to in the content.